International Journal of Applied Mathematics

Volume 38 No. 8s, 2025

ISSN: 1311-1728 (printed version); ISSN: 1314-8060 (on-line version)

WAVELET BASED FAULTY TERMINAL AND PHASE IDENTIFICATION ON HYBRID POWER TRANSMISSION SYSTEM

Kishor P. Jadhav[1*], K. Shivashanker[2*], Srikanth Velpula[3*], S. Chandra Shekar[4*], Dr.Milind P Gajare[5*] and M. S. Saranya[6*]

[1,2]Department of Electrical Engineering, SKN Sinhgad College of Engineering, Korti, Pandharpur, 413 304, Maharashtra, India.

[3]Department of EEE, SR University, Warangal, 506 371, Telangana, India

[4]Department of EEE, NRI Institute of Technology, Agiripalli, 521211, Andhra Pradesh, India

[5]Department of Electronics & Telecommunication,

AISSMS Institute of Information Technology, Pune, India

[6]Department of EEE, Annai Mira College of Engineering and Technology, Ranipet-632517, India

*Corresponding author's Email: kishor.jadhav92921@gmail.com, kondoorushiva@gmail.com, svelpula2020@gmail.com, chandrasekharsavarapu@gmail.com, milind.gajare@aissmsioit.org, sar36892@gmail.com,

Abstract

Efficient fault detection in modern hybrid power transmission systems is crucial due to increasing integration of renewable energy sources and the complexity of long-distance transmission networks. Identifying the faulty phase and terminal rapidly ensures reliable protection and improved power quality. This paper proposes a wavelet-based algorithm using Bior1.5 multi-resolution analysis is used to extract energy coefficients (CD) from post-fault current signals. The discrimination between faulty and healthy phases is achieved by comparing CD values against a threshold derived from simulation data. The method is validated on a 4-bus transmission system under both conventional and hybrid configurations, considering different fault impedances (50 Ω, 250 Ω), locations (4 km, 40 km), and fault inception angles (120°, 340°). Results demonstrate accurate fault phase and terminal identification within 25 ms for symmetrical and unsymmetrical faults, with improved accuracy compared to existing methods. The proposed approach offers robust and fast protection suitable for diverse operating conditions in hybrid power systems.

Keywords: Discrete wavelet transform, Fault detection, Energy coefficients, Hybrid transmission system, Fault inception angle.

Received: August 06 2025

Volume 38 No. 8s, 2025
ISSN: 1311-1728 (printed version); ISSN: 1314-8060 (on-line version)

1. Introduction

The growing demand for electricity has led to the expansion of modern power systems, which now integrate both conventional and non-conventional (renewable) energy sources. Conventional sources, such as thermal and hydro generators, are usually connected through long transmission lines, whereas renewable sources such as solar and wind are often installed closer to load centers. This integration, while improving reliability and reducing transmission losses, introduces significant challenges in protection and fault detection due to differences in generation capacities and fault current levels.

In conventional systems, fault currents are generally large and can be easily detected by traditional protective relays. However, in microgrids and hybrid networks, renewable sources contribute relatively small fault currents, often through power electronic converters. This leads to bidirectional current flow during fault conditions and complicates the reliable operation of protection schemes. As a result, conventional fault detection methods may fail to distinguish between faulty and healthy phases, particularly under high fault impedance or variable fault inception angles. Therefore, advanced protection algorithms are required to ensure selectivity, speed, and accuracy in such diverse operating environments.

Several protection strategies have been proposed in recent literature. Best et al. [4] introduced a three-level protection scheme with breaker communication, though it suffers limitations under low transient fault currents in islanded operation. El-Zonkoly [5] combined wavelet transform with adaptive neural networks but faced challenges in discriminating faults at higher fault resistances. Islam and Gabbar [6] proposed a centralized relay-based microgrid protection method, but it was restricted to microgrid-only configurations. Similarly, Yadav and Swetapadma [7] applied a wavelet-ANN hybrid approach requiring both current and voltage signals, which increases measurement complexity. Other methods such as synchrophasor-based detection [9] or traveling wave techniques [10] often involve high detection times or delayed terminal identification.

These limitations highlight the need for a more reliable and computationally efficient fault detection approach.

Wavelet transform has emerged as a powerful tool for analyzing non-stationary and transient power system signals. Unlike Fourier analysis, wavelets provide both time and frequency localization, making them well-suited for capturing abrupt variations in fault currents. In particular, biorthogonal wavelets such as Bior1.5 offer symmetrical filter properties and accurate feature extraction from transient signals. Energy coefficients (CD), obtained from wavelet decomposition, can be used as fault indicators due to their sensitivity to sudden disturbances.

In this paper, a wavelet-based algorithm using Bior1.5 decomposition is proposed for identifying faulty terminals and phases in a hybrid 4-bus power transmission system. The method relies on extracting and comparing energy coefficients from post-fault current signals. By establishing a threshold between the highest healthy phase value and the lowest faulty phase

Received: August 06 2025

Volume 38 No. 8s, 2025
ISSN: 1311-1728 (printed version); ISSN: 1314-8060 (on-line version)

value, the algorithm effectively discriminates fault locations under a wide range of conditions, including different fault impedances, inception angles, and source capacities. The proposed approach is validated using MATLAB/Simulink simulations on both conventional and hybrid system configurations, and its performance is compared with existing methods [29-30].

The rest of this paper is organized as follows: Section 2 explains the fundamentals of wavelet analysis, Section 3 presents the proposed technique and algorithm, Section 4 discusses the power system model and simulation results, and Section 5 concludes the findings.

2. Wavelets Concept

Wavelet is a small energy wave having finite time interval with energy concentrated over the period. It has scaling ad shifting function and best suited for transient signals having abrupt changing current signals. The wavelet captures the transient signal whenever the signal resolution is match with the wavelet resolution. Hence, it is used for the any type of abrupt changing signal. This analysis is used to give scaling signals from the various frequency bands. The mother wavelet is able to the translated and dilated discretely [11-12]. According to the nature of fault signals the mother wavelet to be chosen to identify the accurate fault detection and classification [13-15]. A Bior1.5 mother wavelet is appropriate for the fault current signals. The Bior1.5 wavelet is a symmetric and has perfect reconstruction property. However, the Wavelet Transform (WT) allows variable window widths (high and low frequencies) to extract the features for the analysis [16]. Wavelets are in the form of series of functions similarly Fourier series [17]. The mother wavelet is represented by:

$$\psi_{j,k}(t) = 2^{\frac{j}{2}}\psi(2^j t - k) \quad (1)$$

$j, k \in Z$

$'Z'$ is an integer number.

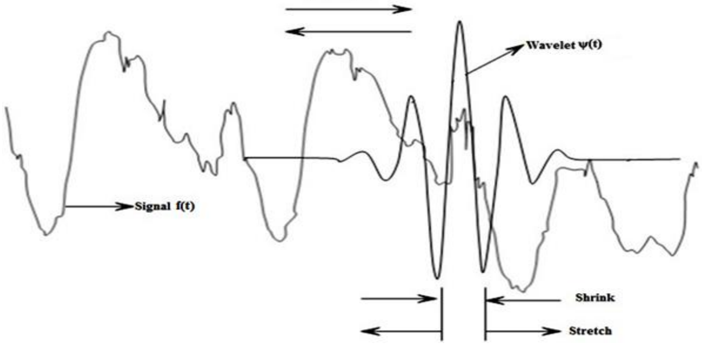

Figure. 1 Transient signal and wavelet.

$'j'$, $'k'$ representing translations and dilations. A high frequency fault signal and bior1.5 wavelet is shown in Fig. 1.

Received: August 06 2025

Volume 38 No. 8s, 2025

ISSN: 1311-1728 (printed version); ISSN: 1314-8060 (on-line version)

A wavelet moves on the transient signal in both forward and reverse direction with shrink and stretch property. It captures the signal wherever both the time and frequency resolution is matched. Later, it extracts the features as CD. Higher abrupt change in the signal generates higher value of CD and vice versa [18]. When a fault occurs, CD of faulted phase has higher value of CD compared to healthy phase [19]. A Bior1.5 wavelet is considered to generate CD from the fault signals [20]. The mathematical expression for DWT [21] is

$$W_{(j,k)} = \int_{-t}^{t} f(t)\ 2^{\frac{j}{2}}\ \psi(2^{j}\, t - k)\ dt \qquad (2)$$

DWT generates good resolution match for the abrupt changing in signals. Many filter applications need symmetrical coefficients as output for achieving linear progress. Other wavelets could not give symmetrical coefficients. Bi-orthogonal wavelet systems can be designed to have symmetrical coefficients [22.]

Let us consider two functions $\Psi(t)$ & $\bar{\Psi}\ (t)$,

$$\bar{\Psi}\ (t) = \sum_{k=o}^{N-1}(-1)^{n}\, h(N-k-1)\bar{\Phi}(2t-k) \qquad (3)$$

$$\Psi(t) = \sum_{K=0}^{N-1}(-1)^{n}\, \bar{h}(N-k-1)\Phi(2t-k) \qquad (4)$$

Calculation of energy coefficient is as follows g(x) is a function.

$$g(x) = \begin{cases} x, & 0 \le x \le 3 \\ 0, & elsewhere \end{cases}$$

The energy coefficient is

$$\beta_{0,0} = \int_{-\infty}^{\infty} g_{0}(x) 2^{0} \Psi(2^{0} x - k) dx$$

$$\beta_{0,0} = \int_{-\infty}^{\infty} g_{0}(x)(1)\Psi(1x - k) dx$$

$$= \int_{0}^{1} x * 1 dx$$

$$= \left. \frac{x^{2}}{2} \right|_{0}^{1}$$

$$= \frac{1}{2}$$

3. Wavelet Based Technique for Faulty Terminal and Phase Identification

The proposed wavelet based technique is designed for extraction of CD from the fault current signals. The post fault current signals are measured at both ends of transmission lines and then

Received: August 06 2025

Volume 38 No. 8s, 2025

ISSN: 1311-1728 (printed version); ISSN: 1314-8060 (on-line version)

compared. In absence of fault, both values are equal otherwise different [23]. This difference is in the form of CD indicates that the fault is occurred. Comparing all the CD a predetermined thresholds value can be fixed to discriminate the faulted and healthy phases [24]. The threshold value is fixed on the basis of CD value i.e. highest value of healthy phase and lowest value of faulty phase [25].

Above the threshold value is considered as faulty phase and below is healthy phase. The flow chart representing the terminal and phase detection of proposed work is shown in Fig. 2.

3.1 Proposed Algorithm

Step-i: Choose any one terminal and apply the fault.
Step-ii: Measure all fault currents of all phases at both the ends.
Step-iii: Wavelet decomposition using bior1.5 on fault current signals.
Step-iv: Obtain CD from the current signals.
Step-v: Get the difference value of CD at both ends.
Step-vi: Get the absolute value of CD of all phases.
Step-vii: Threshold value discriminates fault terminal and the healthy terminal based on absolute values.

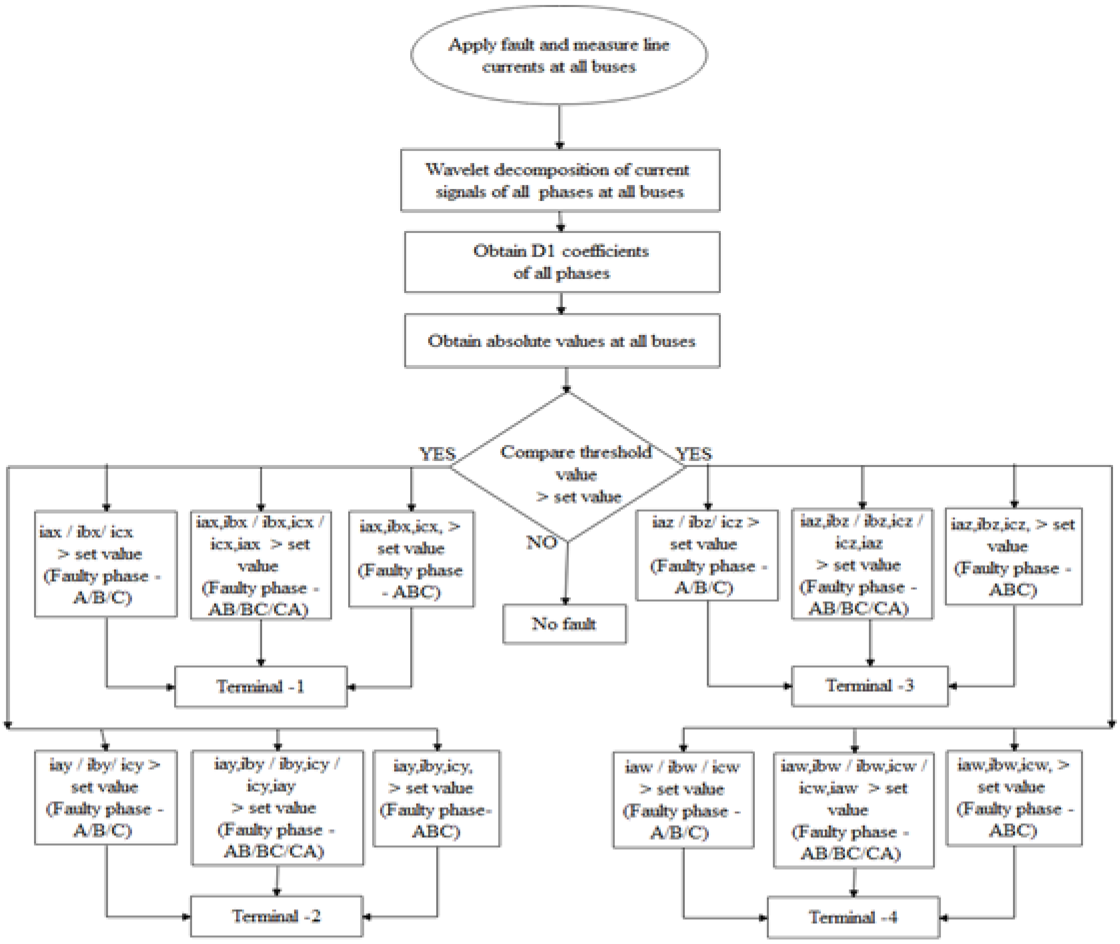

Figure. 2 Flowchart

Received: August 06 2025

International Journal of Applied Mathematics

Volume 38 No. 8s, 2025

ISSN: 1311-1728 (printed version); ISSN: 1314-8060 (on-line version)

4. Power system Model and Result Analysis

A simulation model of 4-bus transmission system is developed on Simulink software for the proposed work. Power system is having 100MVA, 60MVA and 30MVA capacity conventional sources connected to utility grid through 60km distance. A discrete wavelet transforms with Bior1.5 mother wavelet is applied on fault current signals to decompose into CD [26-27]. Results are plotted on fault indices (time in milliseconds on X-axis and CD values on Y-axis).

The fault analysis is carried out on two cases
Case-1: Study of 4-bus conventional sources connected system.
Case-2: Study of 4-bus hybrid sources connected system.

4.1 Case-1: Study of 4-bus conventional sources connected system

A proposed 4-bus transmission system is shown in Fig. 3 for the analysis of various faults with a fault impedance of 250Ω, at distance of 40km at Fault

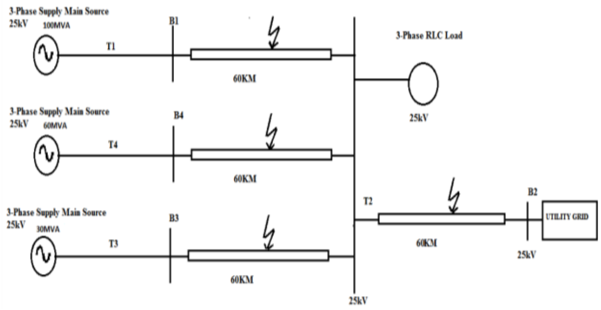

Figure. 3 A 4-bus transmission system.

inception angle (FIA) 340^0.
The proposed system data for the fault analysis of Fig.3 is given as
B1: Power source (100 MVA),
B2: Utility grid (2500 MVA),
B3: Power source (60 MVA),
B4: Power source (30 MVA),
Line distance: 60km each, Frequency: 50Hz.

4.1.1 Fault Analysis

The fault analysis on above proposed system with symmetrical and unsymmetrical faults on terminals T1, T2, T3, and T4 are discussed below.

The fault indices of CD are considered as 4 (faults) x 4 (terminals) =16 sub graphs in which rows indicate energy coefficients of 4 terminals (CD1, CD2, CD3, CD4) and columns indicates 3 phases (a, b, c). As shown in Figures.5,7,9,11, the 1st row 1st column indicates phase-A currents of T1, 1^{st} row 2^{nd} column indicates phase-B currents of T1, 1^{st} row 3^{rd} column indicates phase-C currents of T1 and so on for T2, T3, T4.

Received: August 06 2025

Volume 38 No. 8s, 2025

ISSN: 1311-1728 (printed version); ISSN: 1314-8060 (on-line version)

4.1.2 Results of faults on T1

An LG fault is applied at phase-A at T1 and the fault index of CD1 shown in Fig. 4 and corresponding bar chat is drawn based on highest values of CD1 shown in Fig. 5.

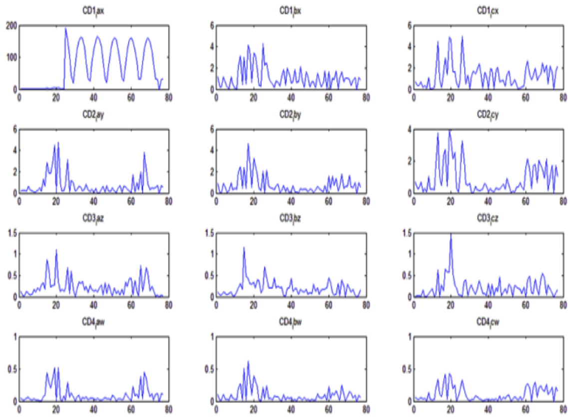

Figure. 4 CD1 LG fault index at T1.

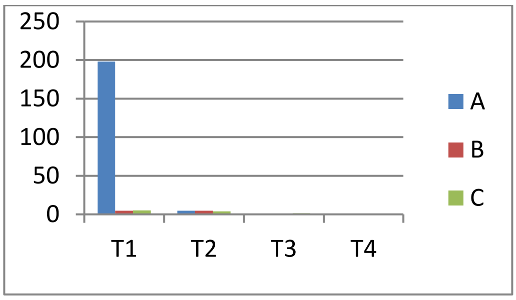

Figure. 5 Faulty terminal (T1) and phases (A)

The Fig. 4 and Fig. 5 revealed that the faulted terminal T1 and fault phase-A has relatively higher values compared to remaining phases of T2, T3, T4. The fault detection time is less than 25msec.

An LLG fault is applied at phase-A, B at T1 and the fault index of CD1 shown in Fig. 6 and corresponding bar chat is drawn based on highest values of CD1 shown in Fig. 7.

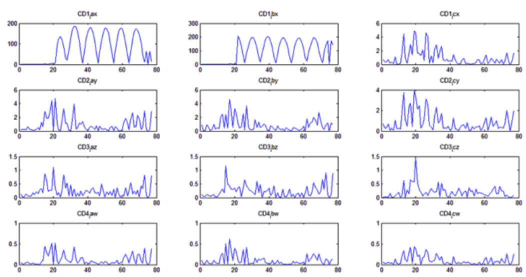

Figure. 6 CD1 LLG fault index at T1.

Received: August 06 2025

International Journal of Applied Mathematics

Volume 38 No. 8s, 2025

ISSN: 1311-1728 (printed version); ISSN: 1314-8060 (on-line version)

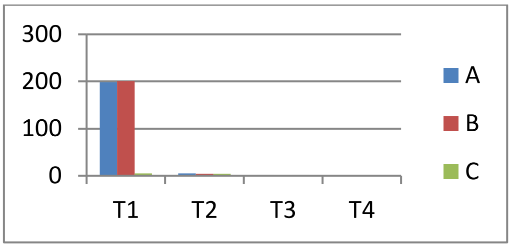

Figure. 7 Faulty terminal (T1) and phases (A, B).

The Fig. 6 and Fig. 7 revealed that the faulted terminal T1 and fault phase-A, B has relatively higher values compared to remaining phases of T2, T3, T4. The fault detection time is less than 25msec.

An LL fault is applied at phase-A, B at T1 and the fault index of CD1 shown in Fig. 8 and corresponding bar chat is drawn based on highest values of CD1 shown in Fig. 9.

	A	B	C
T1	**198**	**201**	4.94
T2	4.62	4.04	4.5
T3	1.44	1.15	1.42
T4	0.49	0.65	0.38

Figure. 8 CD1 LL fault index at T1.

The Fig.8 and Fig.9 revealed that the faulted terminal T1 and fault phase-A, B has relatively higher values compared to remaining phases of T2, T3, T4. The fault detection time is less than 25msec.

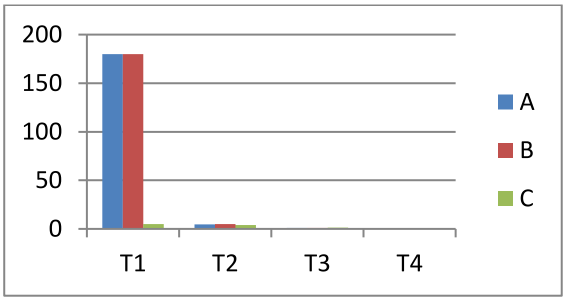

Figure. 9 Faulty terminal (T1) and phases (A, B).

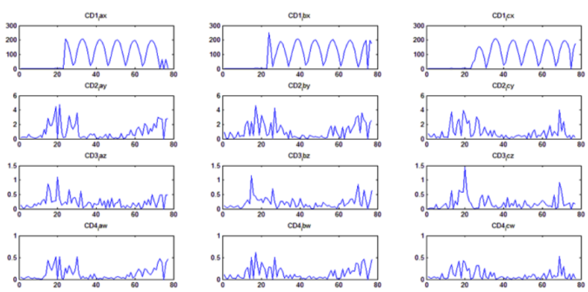

Figure. 10 CD1 3-phase fault index at T1.

Received: August 06 2025

Volume 38 No. 8s, 2025
ISSN: 1311-1728 (printed version); ISSN: 1314-8060 (on-line version)

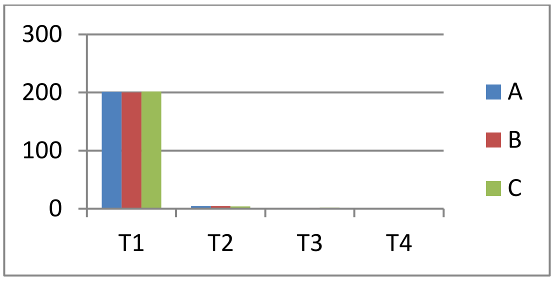

Figure. 11 Faulty terminal (T1) and phases (A, B, C).

A 3-phase fault is applied at phase-A, B, C at T1 and the fault index of CD1 shown in Fig. 10 and corresponding bar chat is drawn based on highest values of CD1 shown in Fig. 11.

The Fig. 10 and Fig. 11 revealed that the faulted terminal T1 and fault phase-A, B has relatively higher values compared to remaining phases of T2, T3, T4. The fault detection time is less than 25msec.

It is observed from the Fig. 5, 7, 9 and Fig. 11 the CD1 of faulty terminal highest values are 200, 200, 180, 202 respectively and the CD1 of healthy terminal highest values are 4.97, 4.94, 4.8 and 4.49 respectively. So that, it is seen the discrimination of faulty and healthy terminal can be clearly noticed. The highest CD1 of all phases at all terminals with all faults are summarised in Table. 1.

Table. 1. CD1 summary of fault at T1

Type of Fault	Terminal											
	T1			T2			T3			T4		
	A	B	C	A	B	C	A	B	C	A	B	C
LG	198	4.97	4.94	4.2	4.0	4.9	1	1	1.5	0.5	0.5	0.4
LLG	198	200	4.8	4.6	4.5	4.5	1	1.2	1.5	0.5	0.5	0.4
LL	180	180	4.49	4.1	4.2	4.3	1	1.2	1.5	0.5	0.5	0.4
3-phase	201	200	202	4.3	4.1	3.5	1	1.2	1.5	0.5	0.5	0.4

It has been observed from Table. 1 at T1 the highest value is 202 and the lowest value is 180 on fault terminal whereas highest value is 4 and the lowest value is 0 among all healthy terminals. Therefore, the threshold value can be fixed between the values 4 to 180 as discussed in section-3. Above the threshold value is considered as faulty phase and below is healthy phase. Similarly, analysis is carried out on all remaining terminals and the results are summarised in Table 2.

Table. 2. CD summary of fault at all terminals

Received: August 06 2025

ISSN: 1311-1728 (printed version); ISSN: 1314-8060 (on-line version)

Type of Fault	Terminal											
	T1			T2			T3			T4		
	A	B	C	A	B	C	A	B	C	A	B	C
LG	198	4	4	130.0	4.24	0.91	1.45	2.08	310	0.70	180.0	0.75
LLG	198	200	4	6.01	180.1	198.5	198	1.08	311	155.0	0.84	311.6
LL	180	180	4	0.5	198	198	200	0.5	200	120	0.5	120
3-phase	201	200	202	198.6	197.0	200.0	148	150	200	160.0	180.0	351.05

4.2 Case-2: Study of 4-bus hybrid sources connected system

The proposed 4-bus hybrid power transmission system shown in Fig. 12 is considered for the analysis of different types of faults with a fault impedance of 50Ω, at a distance of 40km and Fault inception angle (FIA) 1200. A Wind system and solar PV system are integrated at bus-3 and bus-4 respectively to the PCC through a 6km line instead of the 60km line by replacing the conventional generators.

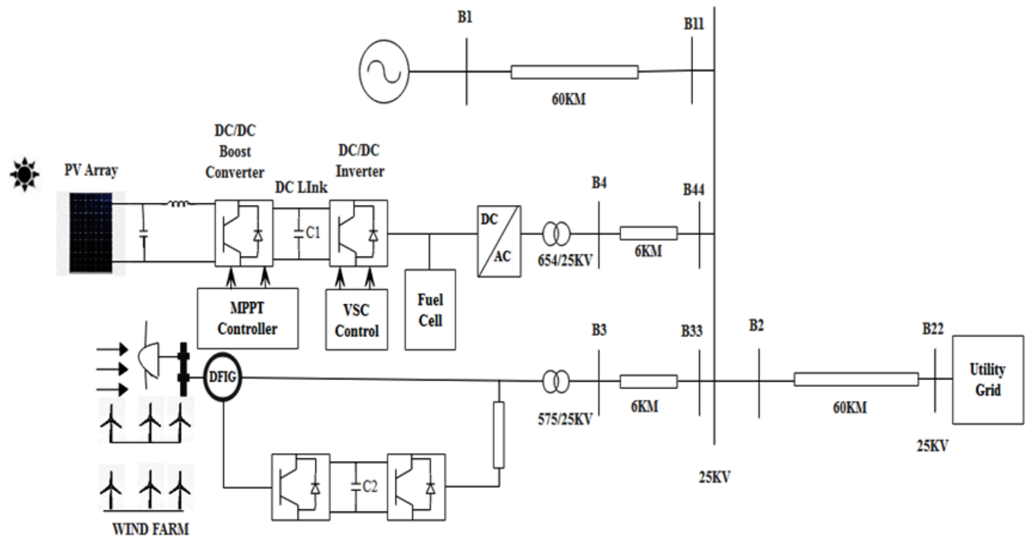

Figure. 12 A 4-bus hybrid power transmission system.

The proposed system data for the fault analysis is given as:

B1: Main generator (100 MVA),
B2: Grid (2500 MVA),
B3: Wind power (10 MW),
B4: Solar PV (1MW),
Fuel cell parameters (50KW), Transmission lines distance: 60km each, Frequency: 50Hz.

Received: August 06 2025

Volume 38 No. 8s, 2025

ISSN: 1311-1728 (printed version); ISSN: 1314-8060 (on-line version)

4.2.1 Results of fault on T3

Apply LG, LLG, LL, 3-phase faults on various phases at T3 and obtain fault indices of CD3.

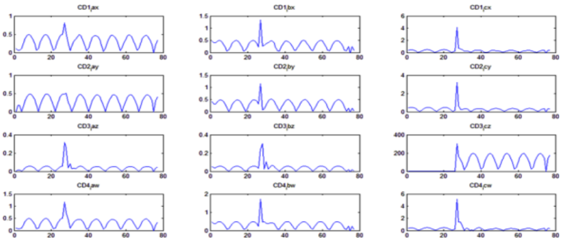

Figure. 13 CD3 LG fault index at T3

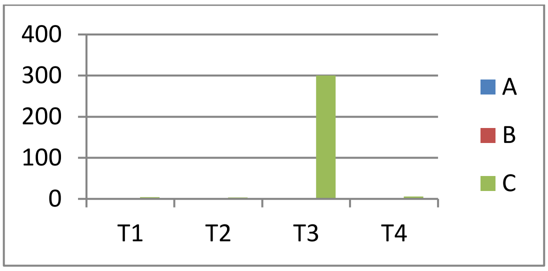

Figure. 14 Faulty terminal (T3) and phases (C)

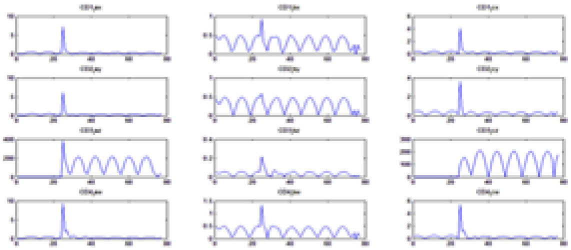

Figure. 15 CD3 LLG fault index at T3

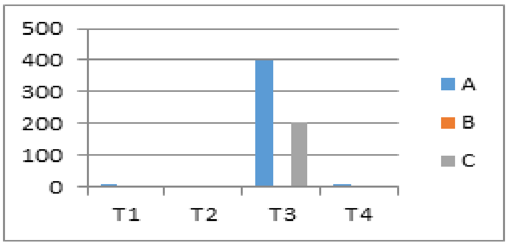

Figure. 16 Faulty terminal (T3) and phases (A, C).

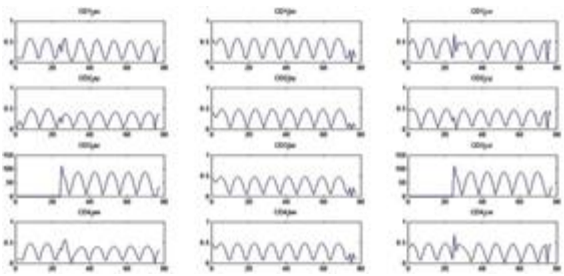

Figure. 17 CD3 LL fault index at T3.

Received: August 06 2025

Volume 38 No. 8s, 2025

ISSN: 1311-1728 (printed version); ISSN: 1314-8060 (on-line version)

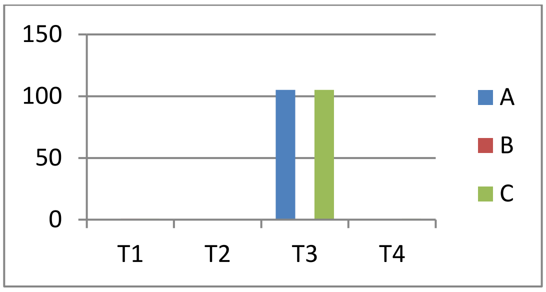

Figure. 18 Faulty terminal (T3) and phases (A, C).

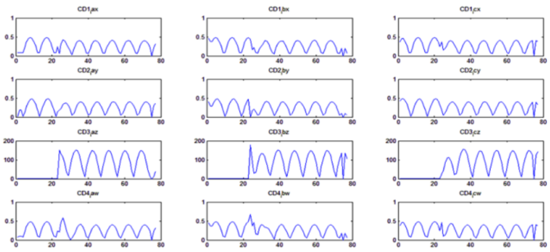

Figure. 19 CD3 LLLG fault index at T3

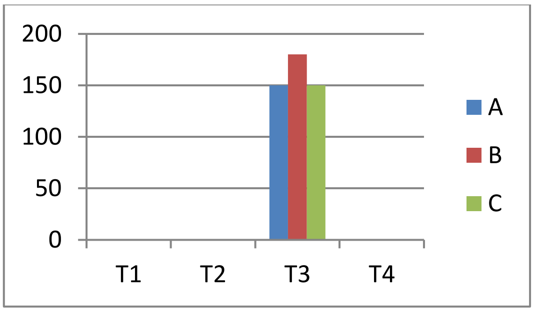

Figure. 20 Faulty terminal (T3) and phases (A, B, C).

It is observed from the Fig.14, 16, 18 and Fig. 20 the CD3 of faulty terminal highest values are 302, 398, 115, 190 respectively and the CD3 of healthy terminal highest values are 7.1, 5.2, 9.1 respectively. So that, it is seen the discrimination of faulty and healthy terminal can be clearly noticed. The highest CD3 of all phases at all terminals with all faults are summarised in Table. 3.

Table.3. CD3 summary of fault at T3

Type of Fault	Terminal											
	T1			T2			T3			T4		
	A	B	C	A	B	C	A	B	C	A	B	C
LG	0.8	1.35	4.1	0.5	1.1	3.7	0.32	0.34	**302**	1.2	1.8	4.5

Received: August 06 2025

ISSN: 1311-1728 (printed version); ISSN: 1314-8060 (on-line version)

LLG	7.1	0.9	4.1	5.2	0.51	3.8	**398**	0.3	**202**	9.1	1.4	5.8
LL	0.5	0.5	0.5	0.5	0.5	0.5	**115**	0.5	**115**	0.55	0.5	0.6
3-phase	0.5	0.5	0.5	0.5	0.5	0.5	**152**	**190**	**160**	0.6	0.7	0.49

4.2.2 Results of fault on T4

Apply LG, LLG, LL, 3-phase faults on various phases at T4 and obtain fault indices of CD4.

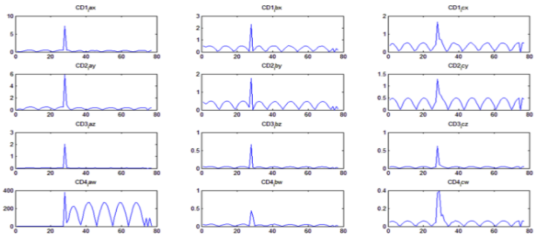

Figure 21. CD4 LL fault index at T4

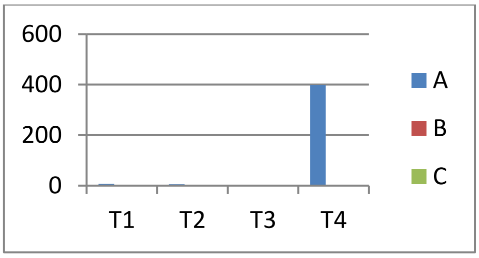

Figure 22. Faulty terminal (T4) and phases (A)

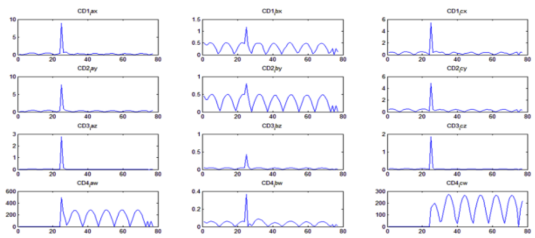

Figure 23. CD4 LL fault index at T4

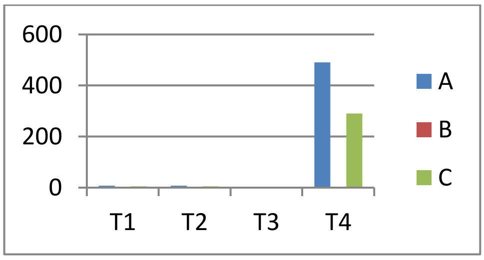

Figure 24. Faulty terminal (T4) and phases (A, C)

Received: August 06 2025

International Journal of Applied Mathematics

Volume 38 No. 8s, 2025

ISSN: 1311-1728 (printed version); ISSN: 1314-8060 (on-line version)

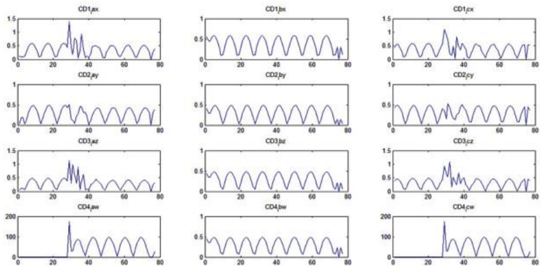

Figure 25. CD4 LL fault index at T4

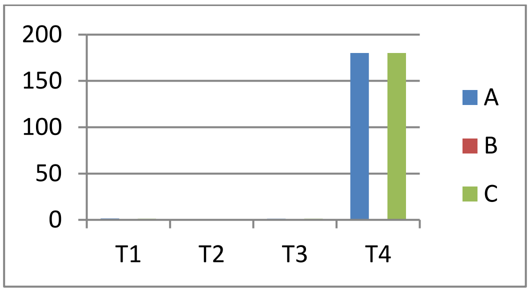

Figure 26. Faulty terminal (T4) and phases (C)

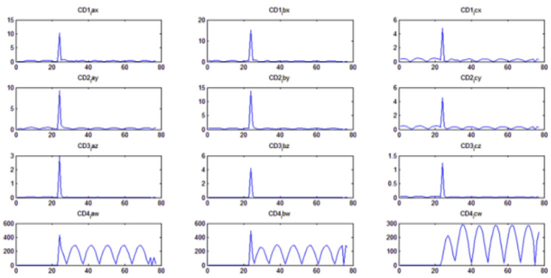

Figure 27. CD4 LL fault index at T4

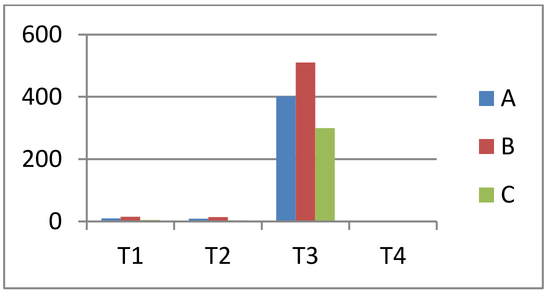

Figure 28. Faulty terminal (T4) and phases (A, B, C)

It is observed from the Fig. 22, 24, 26 and Fig. 28 the CD4 of faulty terminal highest values are 390, 490, 180, 470 respectively and the CD4 of healthy terminal highest values are 10,9,4, respectively. So that, it is seen the discrimination of faulty and healthy terminal can be clearly noticed. The highest CD4 of all phases at all terminals with all faults are summarised in Table. 4.

The proposed algorithm is compared with existing method [28] of terminal identification is shown in Table.5.

Received: August 06 2025

Volume 38 No. 8s, 2025

ISSN: 1311-1728 (printed version); ISSN: 1314-8060 (on-line version)

Table.4. CD4 summary of fault at T4

Type of Fault	Terminal											
	T1			T2			T3			T4		
	A	B	C	A	B	C	A	B	C	A	B	C
LG	7.1	2.4	1.7	6	1.8	1.4	2.1	0.7	0.7	390	0.4	0.4
LLG	8.2	1.2	5.8	7.2	0.7	4.8	2.8	0.45	1.8	490	0.3	280
LL	1.4	0.5	1.1	0.5	0.5	0.5	1.1	0.5	1.1	180	0.5	180
3-phase	10	15	4.9	9	14	4.2	3	4	1.1	401	470	300

Table.5. Comparison of proposed method with Existing method for variation in terminal identification

S.No	**Parameter**	**Existing method [28]**	**Proposed method**	**Observations**
1	Fault classification accuracy	96.08% accuracy	98.55% accuracy	better accuracy
2	Effect of fault impedance	does not work effectively above 200Ω	do not effect up to 300Ω	considerably better
3	Fault inception angle	does not work effectively when exceeds 330^0	works well for all Fault inception angles	Good performance

5. Conclusion

This study presented a wavelet-based method for fault terminal and phase identification in a 4-bus hybrid power transmission system. By applying Bior1.5 wavelet decomposition to fault current signals, energy coefficients (CD) were extracted and used to discriminate faulty phases and terminals from healthy ones. Simulation results on both conventional and hybrid systems

Received: August 06 2025

Volume 38 No. 8s, 2025

ISSN: 1311-1728 (printed version); ISSN: 1314-8060 (on-line version)

confirmed accurate detection of LG, LLG, LL, and three-phase faults. The method achieved discrimination within 25 ms, regardless of variations in generation capacity, fault inception angle, fault impedance, or distance. Compared with existing approaches, the proposed technique demonstrated higher accuracy, better tolerance to fault impedance, and faster detection. These features make it a reliable solution for modern hybrid grids. Future work may focus on extending the algorithm to large-scale networks and validating its performance under real-time hardware implementation.

Conflicts of Interest

The authors declare no conflict of interest.

References

[1] S. Karan and H. G. Yeh, " Fault Classification in Microgrids using Deep Learning", In: Proc. of IEEE Green Energy and Smart Systems Conference (IGESSC), Long Beach, CA, USA, pp. 1-7, 2020

[2] S. K. Prince, S. Affijulla and G. Panda, "Protection of DC Microgrids Based on Complex Power During Faults in On/Off-Grid Scenarios", IEEE Transactions on Industry Applications, Vol. 59, No. 1, pp. 244-254, Feb. 2023

[3] T. Khalili and A. Bidram, "*Distributed Control Approaches for Microgrids*", Springer International Publishing, pp. 275-288, 2021

[4] R. J. Best, D. J. Morrow and P. A. Crossley, "Communication assisted protection selectivity for reconfigurable and islanded power networks", In: Proc. of 44th International Universities Power Engineering Conference (UPEC), Glasgow, UK, pp. 1-5, 2009

[5] A.M. El-Zonkoly, H. Desouki, “Wavelet entropy based algorithm for fault detection and classification in FACTS compensated transmission line”, International Journal of Electrical Power & Energy Systems, Vol. 33, No. 8, pp. 1368-1374, 2011

[6] Md Razibul Islam and Hossam A. Gabbar, " Study of Micro Grid Safety & Protection Strategies with Control System Infrastructures ", Smart Grid and Renewable Energy, Vol. 3, pp. 1-9, Jan. 2012

[7] A. Yadav and A. Swetapadma, “A single ended directional fault section identifier and fault locator for double circuit transmission lines using combined wavelet and ANN approach”, International Journal of Electrical Power & Energy Systems, Vol. 69, pp. 27-33, 2015

[8] T. Bakir, B. Boussaid, R. Hamdaoui, M. N. Abdelkrim and C. Aubrun, "Fault detection in wind turbine system using wavelet transform: Multi-resolution analysis", In: Proc. of IEEE 12th International Multi-Conference on Systems, Signals & Devices (SSD15), Mahdia, Tunisia, pp. 1-6, 2015

Received: August 06 2025

ISSN: 1311-1728 (printed version); ISSN: 1314-8060 (on-line version)

[9] M. Pignati, L. Zanni, P. Romano, R. Cherkaoui and M. Paolone, " Fault Detection and Faulted Line Identification in Active Distribution Networks Using Synchrophasors-Based Real-Time State Estimation ", IEEE Transactions on Power Delivery, Vol. 32, No. 1, pp. 381-392, Feb. 2017

[10] Z. Yi and A. H. Etemadi, "Fault Detection for Photovoltaic Systems Based on Multi-Resolution Signal Decomposition and Fuzzy Inference Systems", IEEE Transactions on Smart Grid, Vol. 8, No. 3, pp. 1274-1283, May 2017

[11] H. Alberto Jimenez and D. Guillen and R. Tapia-Olvera and Gerardo Escobar and F. Beltran-Carbajal, " An improved algorithm for fault detection and location in multi-terminal transmission lines based on wavelet correlation modes ", Electric Power Systems Research, Vol. 192, 2021

[12] A. S. Veerendra, A. A. Shah, and M. R. Mohamed, C. P. Sekhar, and P. Leung, "Wavelet Transform Based Fault Identification and Reconfiguration for a Reduced Switch Multilevel Inverter Fed Induction Motor Drive", Electronics, Vol. 10, No. 9, 2021

[13] M. Zamorano and M. J. Gómez Garcia and C. Castejón, " Selection of a mother wavelet as identification pattern for the detection of cracks in shafts", Journal of Vibration and Control, Vol. 28, No. 21-22, pp. 3152-3161, 2022

[14] W. K. Ngui, M. S. Leong, and L. M. Hee, and A. M. Abdelrhman, " Wavelet Analysis: Mother Wavelet Selection Methods", In: Proc. of Applied Mechanics and Materials, Vol. 393, pp. 953-958, Nov. 2013

[15] A. R. Adly, R. A. El Sehiemy and A. Y. Abdelaziz, "A novel single end measuring system based fast identification scheme for transmission line faults", Measurement, Vol. 103, pp. 263–274, 2017

[16] N. S. Wani, R. P. Singh and M. U. Nemade "Detection, Classification and Localization of Faults of Transmission Lines using Wavelet Transform and Neural Network", In: Proc. of International Journal of Applied Engineering Research, Vol. 13, No. 1, pp. 98-106, 2018

[17] K. P. Soman, K. I. Ramachandran, N. G. Resmi "*Insight into wavelets from theory to practice*" PHI publications, 3rd edition, 2010

[18] D. Onufriienko, Y. Taranenko, " Filtering and Compression of Signals by the Method of Discrete Wavelet Decomposition into One-Dimensional Series", Cybernetics and Systems Analysis, pp. 331-338, Vol. 59, No. 2, 2023

[19] T. Zhang, K. Han, H. Li, S. Liu and F. Chen, "Two terminals protection method for HVDC transmission lines based on maximal overlap discrete wavelet transform and cross-correlation coefficient of traveling wave", Energy Reports, Vol. 9, No. 7, pp. 1133-1148, 2023

Received: August 06 2025

Volume 38 No. 8s, 2025

ISSN: 1311-1728 (printed version); ISSN: 1314-8060 (on-line version)

[20] C. A. Micchelli and Y. Yu, “Reconstruction and Decomposition Algorithms for Biorthogonal Multi-Wavelets”, Multidimensional Systems and Signal Processing, Vol. 8, No. 1-2, pp. 31-69, 1997

[21] M. Geethanjali and K. Priya, " Combined wavelet transforms and neural network (WNN) based fault detection and classification in transmission lines", Elixir International Journal of Electrical Engineering, pp. 3817-3824, Jan. 2009

[22] C. S Burrus, R. A. Gopinath, and H. Guo “Introduction to Wavelets and Wavelet Transforms”, *Upper Saddle River, N. J.: Prentice Hall*, 1998

[23] K, Krishna, V. Vanitha, M. Hussien and G. Mohamed, “Framework for Transmission Line Fault Detection in a Five Bus System Using Discrete Wavelet Transform”. Distributed Generation & Alternative Energy Journal, Dec. 2021

[24] A. Pragati, D. A. Gadanayak and M. Mishra, "Fault detection and fault phase identification in a VSC-MT-HVDC link using Stockwell transform and Teager energy operator", Electric Power Systems Research, Vol. 236, Nov. 2024

[25] J. Uday Bhaskar and S.S Tulasi Ram, "Wavelet- Fuzzy Based Multi Terminal Transmission System Protection Scheme in the Presence of STATCOM Controller", International Journal of Fuzzy Logic Systems (IJFLS), Vol. 6, No. 3, July 2016

[26] R. K. Goli, R. Devi Neerukonda, R. Ganji, M. Bethala, L. S. S. Mallika.K and P. Golla, “Wavelet Based Microgrid Protection in Presence of UPFC using Machine Learning Approach”, In: Proc. of IEEE International Conference on Electronics, Computing and Communication Technologies (CONECCT), Bangalore, India, pp. 1-6, 2024

[27] G. Amit Kumar and A. Gafoor Shaik, " k-Nearest neighbour based approach for the protection of distribution network with renewable energy integration", Electric Power Systems Research, Vol. 220, 2023.

[28] S.Chandra Shekar, G.Ravi Kumar, S.V.N.L Lalitha “Renewable energy integrated multi-terminal transmission system using wavelet based protection scheme” International Journal of Power Electronics and Drive System (IJPEDS) Vol.10, No.2, June 2019, pp. 995~1002.

[29] Swami, S. S., & Mulani, A. O. (2017, August). An efficient FPGA implementation of discrete wavelet transform for image compression. In 2017 International Conference on Energy, Communication, Data Analytics and Soft Computing (ICECDS) (pp. 3385-3389). IEEE.

[30] Kulkarni, P., & Mulani, A. O. (2015). Robust invisible digital image watermarking using discrete wavelet transform. International Journal of Engineering Research & Technology (IJERT), 4(01), 139-141.

Received: August 06 2025

ISSN: 1311-1728 (printed version); ISSN: 1314-8060 (on-line version)

[31] A. Bhagwat, S. Dutta, V. K. Jadoun, A. S. Veerendra, S. K. Sahu, " A customised artificial neural network for power distribution system fault detection", IET Generation, Transmission & Distribution, Vol. 18, No. 11, pp. 2105–2118, 2024

[32] Mulani, A. O., & Mane, P. B. (2017). Watermarking and cryptography based image authentication on reconfigurable platform. Bulletin of Electrical Engineering and Informatics, 6(2), 181-187.

[33] Swami, S. S., & Mulani, A. O. (2017, August). An efficient FPGA implementation of discrete wavelet transform for image compression. In 2017 International Conference on Energy, Communication, Data Analytics and Soft Computing (ICECDS) (pp. 3385-3389). IEEE.

[34] Kulkarni, P. R., Mulani, A. O., & Mane, P. B. (2016). Robust invisible watermarking for image authentication. In Emerging Trends in Electrical, Communications and Information Technologies: Proceedings of ICECIT-2015 (pp. 193-200). Singapore: Springer Singapore.

[35] Mulani, A. O., & Mane, P. B. (2016). Area efficient high speed FPGA based invisible watermarking for image authentication. Indian journal of Science and Technology, 9(39), 1-6.

[36] Mulani, A. O., & Mane, D. P. (2017). An Efficient implementation of DWT for image compression on reconfigurable platform. International Journal of Control Theory and Applications, 10(15), 1-7.

[37] Mulani, A. O., & Mane, P. (2018). Secure and area efficient implementation of digital image watermarking on reconfigurable platform. International Journal of Innovative Technology and Exploring Engineering, 8(2), 56-61.

[38] Takale, S., & Mulani, A. (2022). DWT-PCA based video watermarking. Journal of Electronics, Computer Networking and Applied Mathematics (JECNAM) ISSN, 2799-1156.

[39] Kulkarni, P., & Mulani, A. O. (2015). Robust invisible digital image watermarking using discrete wavelet transform. International Journal of Engineering Research & Technology (IJERT), 4(01), 139-141.

[40] Shinde, M. R. S., & Mulani, A. O. (2015). Analysisof biomedical image using wavelet transform. International Journal of Innovations in Engineering Research and Technology, 2(7), 1-7.

[41] Mane, D. P., & Mulani, A. O. (2019). High throughput and area efficient FPGA implementation of AES algorithm. International Journal of Engineering and Advanced Technology, 8(4).

Received: August 06 2025